

DC component analysis at LWA1

December 17, 2013

Frank Schinzel & Jayce Dowell (UNM)

1 Introduction

After the newly constructed LEDA¹ outriggers at LWA1 became operational Hank Tillman and Steve Ellingson performed TBN observations on September 5, 2013. They only looked at the 5 outriggers and performed dipole-dipole correlations for those baselines. They noted discrepancies in the magnitude and phase of the correlation products going from baseline to baseline. More importantly they reported a strong DC offset/component in the fringe rate plots for most of the baselines that desensitizes them to the point that they are not useable as-is. This initial report led to the detailed analysis of the situation documented in this memo.

The initially observed strong DC components can have different origins. On a system intrinsic level, signal cross-talk as well as common modes can be the cause of strong DC components. Externally, they could be caused by e.g. strong RFI hitting two dipoles at the same time or mutual sky correlation of nearby dipoles. Initial investigation of strong DC components found in cross-correlation of individual dipoles from TBN captures revealed a persistent pattern of high DC components from correlations of dipoles with signal paths going through adjacent channels on a given ARX board. This led to the conclusion that enhanced cross-talk is present for signals using the same RJ45 output of the ARX board that results in most cases in a dramatically increased DC component when correlating those signals with each other. In order to mitigate this effect for the outriggers the signal paths of the outriggers were separated to use five different RJ45 cables. The mapping in the LWA1 SSMIF file was updated to account for this recabling (SSMIF version from October 31, 2013).

The baseline combinations of all five outriggers were used for subsequent analysis of the DC component of correlations between outriggers in order to verify the integrity of the signal paths and that no significant cross-talk or common mode is affecting data quality.

¹<http://www.ledatelescope.org>

Table 1 lists the current cable mapping for the LEDA64 antennas corresponding to the SSMIF version from October 31, 2013. Figure 1 illustrates the LEDA64 configuration with the outriggers labeled accordingly.

Table 1: Current LEDA64 signal path mapping.

Out-rigger #	Stand #	ARX Stand	Split-ter	Box Input	ARX Brd	ARX Chan-nel	DP Patch Cable	LEDA Corr. Input	Comment
	229	241	3	A	140	1/2	Long	0	
	154	242	3	A	140	3/4	Long	2	
2	260	259	3	B	137	1/2	Short	4	
	198	260	3	B	137	3/4	Short	6	
	207	225	3	C	123	1/2	Short	8	
	215	226	3	C	123	3/4	Short	10	
	18	219	3	D	139	5/6	Short	12	
	252	220	3	D	139	7/8	Short	14	
3	259	57	2	A	136	1/2	Long	16	
	121	58	2	A	136	3/4	Long	18	
	20	183	2	B	115	13/14	Long	20	
1	257	184	2	B	115	15/16	Long	22	
5	35	65	2	C	129	1/2	Long	24	
	108	66	2	C	129	3/4	Long	26	
	203	261	2	D	137	5/6	Long	28	
4	258	262	2	D	137	7/8	Long	30	RTA
	157	25	4	A	130	1/2	Long	48	
	174	26	4	A	130	3/4	Long	50	
	226	37	4	B	138	9/10	Long	52	
	240	38	4	B	138	11/12	Long	54	
	127	29	4	C	130	9/10	Long	56	
	153	30	4	C	130	11/12	Long	58	
	123	13	4	D	101	9/10	Short	60	dead y-pol
	172	14	4	D	101	11/12	Short	62	
	253	231	1	A	123	13/14	Short	32	
	6	232	1	A	123	15/16	Short	34	
	255	227	1	B	123	5/6	Short	36	
	64	228	1	B	123	7/8	Short	38	
	12	129	1	C	114	1/2	Short	40	
	42	130	1	C	114	3/4	Short	42	
	250	199	1	D	141	13/14	Short	44	
	114	200	1	D	141	15/16	Short	46	

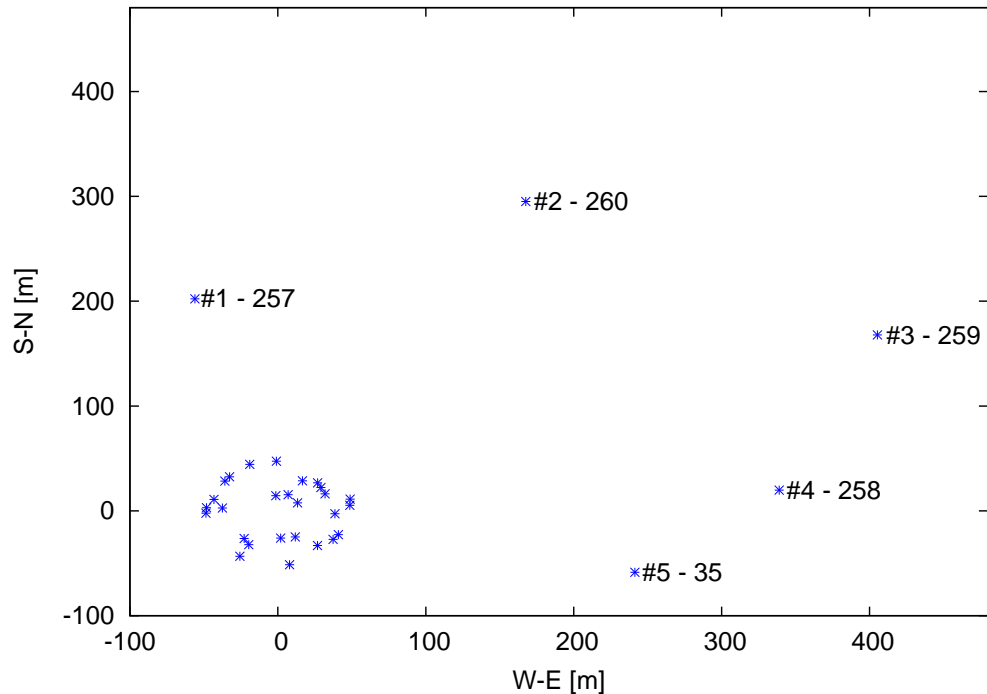


Figure 1: Configuration of the LEDA64 stands with the outrigger stand numbers marked for reference.

2 Observations from October 31 2013

A four hour TBN capture was taken between UT 00:15 and 04:15 on October 31, at 74.0 MHz which included the transits of Cyg A and Cas A. The data were correlated for the following stand baseline combinations: 257, 258, 259, 260, 108, 35 (selecting all outriggers) and stand number 108 from the core array which has an adjacent signal path with stand 35. The correlation was performed with LSL version 0.6.5 using `lsl.correlator.fx.FXMaster` with no gain correction applied. The resulting visibilities are then Fourier transformed using the numpy implementation of a FFT to obtain the fringe rate spectrum. From the fringe rate spectra the 0 Hz value (i.e. DC component) was extracted and is plotted in Figure 2 for all baselines investigated.

Inspection of the DC component amplitudes we find three baselines that show unusually high values in XX polarization, which corresponds to East-West on the sky. These baselines are 257-260, 258-259, and 108-35. 108-35 can be explained by cross-talk due to the signal

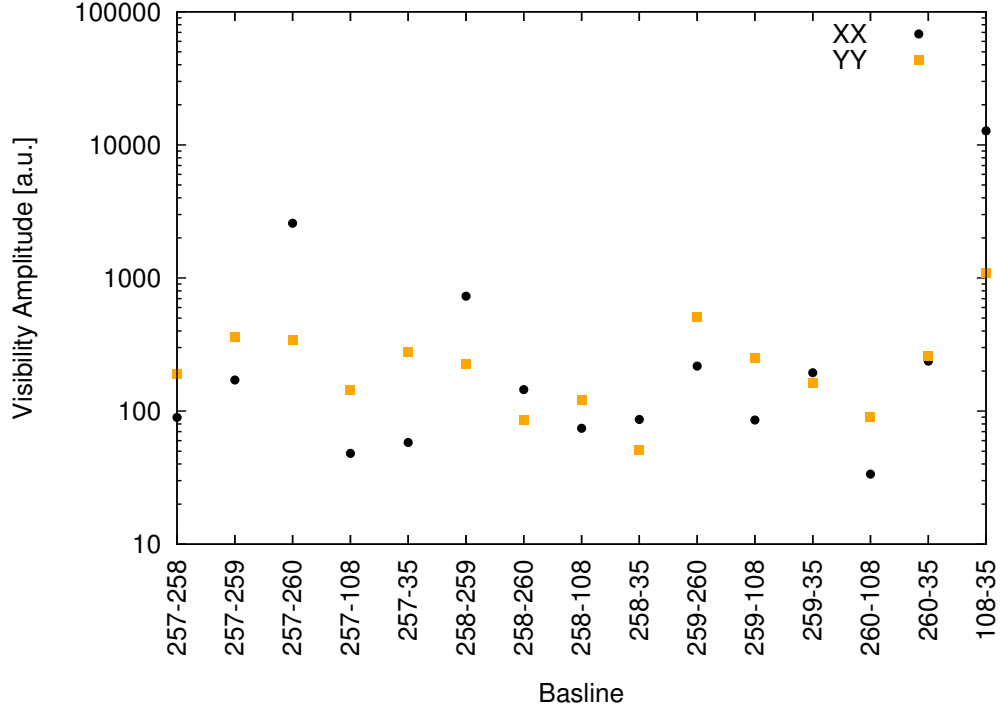


Figure 2: DC component values for all outrigger baselines and stand #108.

paths for those outriggers being on a single RJ45 cable. However, interesting to note is that there is a significant difference between the XX and YY polarizations which is unexplained. Baseline 257-260 have completely different signal paths, with the exception of being powered through the same frontend power controller board. There seems to be no clear reason for such a high DC component if it were caused by the instrument. Baseline 258-259 has in comparison a smaller DC component but still visibly higher than most of the baselines. Also in this case the signal paths are completely different.

The baseline 108-258 is similar to the observation conducted for LWA Memo #186. There a fringe rate plot for a dipole-dipole correlation is shown in Figure 9, which is reproduced here on the right in Figure 3. On the left in Figure 3 the visibility amplitude, phase, and fringe rate for the 108-258 baseline is shown. Visual comparison of the two fringe rate plots shows that the DC component is found to be of similar magnitude in comparison to Cyg A and Cas A. The larger differences in the fringe rate plot are due to the different integration times resulting in different fringe rate resolutions. The dataset from LWA Memo #186 has a duration of 3500s within which Cyg A and Cas A both transit. The DC component in this case is explained in LWA Memo #166 as the “all sky” contribution. The observation discussed here has a duration of 16000s, which causes the fringe rate peaks to wash out and adds a contribution from the Galactic plane.

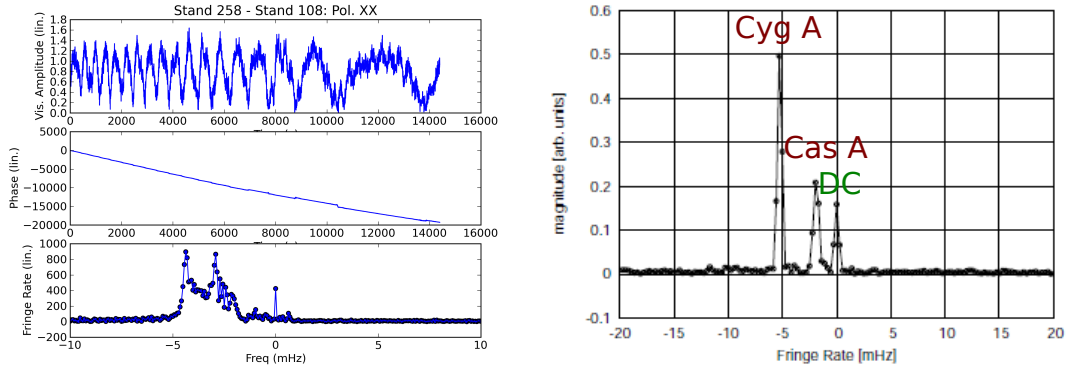


Figure 3: Left shows the amplitude, phase, and fringe rate for the XX polarization of the 108-258 baseline, the YY polarization looks similar. On the right is Fig. 9 of LWA Memo #186, showing a similar fringe rate plot.

3 Investigation of all LEDA64 baselines

Further analysis of all baselines for the stands listed in Table 1 revealed that no signal was found on stand #123 E-W polarization. Physical investigation of the signal path showed that the frontend and signal path work and that most likely a dead ASP channel or faulty wiring after entry into the ASP rack is responsible for this. This will be addressed by future maintenance work.

The following observations were made from looking at all LEDA64 baselines:

1. A particularly high DC component is observed from baselines with their signal paths sharing the same RJ45 cable. Especially the XX polarization seems to be affected by this.
2. Spurious high DC component values were found for baselines that especially include outriggers #1, #2, and #3, as well as stand #198.
3. Nearby dipoles, i.e. short baselines, have a stronger DC component (not unexpected, see LWA Memo #166).

In order to remove some of the contaminants, a plot of DC components from all baselines was made excluding baselines of stand #123 and #198 and removing all baselines sharing the same RJ45 connector. A plot of the resulting DC components is shown in Fig. 4.

The higher DC component from short baselines is due to sky noise correlation, however there are a bunch of other spurious baselines with high DC components. Looking at them they have one of the ouriggers #1, #2, or #3 as one of their elements. Another baseline distance plot removing baselines with outriggers #1 and #2 was produced (Fig. 4 right). It is clearly much cleaner on the longer baselines. The high points in YY are outrigger #3 baselines.

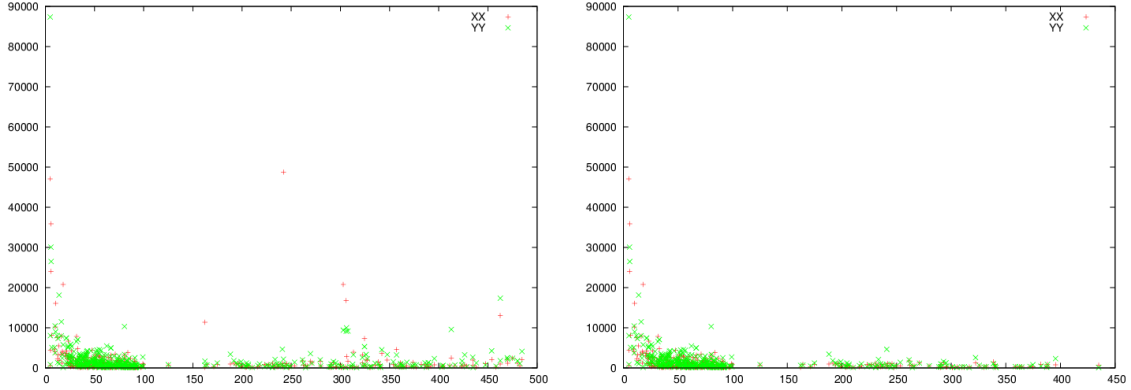


Figure 4: Left: DC component plotted against baseline length in m for all LEDA64 baselines except those that include stands #123 and #198. Right: Same as left plot but baselines with outrigger #1 and #2 were removed.

Strangely, not all baselines from outrigger #1, #2, and #3 are affected by the strong DC component, which is puzzling and rules out common mode within the ASP rack. There is no reason for a correlation between those baselines other than external influence. To better visualize the spatial distribution of high DC component values, a 3D representation (2D projection) at the mid-point of each baseline was plotted ($x=x_0-dx/2$, $y=y_0-dy/2$, $z=DC$ power). Interestingly, the plot can be rotated so that the points of high DC components line up along a particular plane and produce vertical bars. It looks like there are certain distances in the (u,v) -plane that show high DC components, which reminds of powerline RFI with bursts sweeping across the array. The orientation matches a NE or SW geometry consistent with this suspicion. Due to the interactive nature of this plotting method no Figure was added demonstrating this.

There is no evidence of power line spikes in the TBN short time series data, which does not exclude this scenario since the inherently narrow bandwidth of the TBN is not sensitive enough to short broadband spikes. What seems to be the case is, if there is a strong DC component then there is also a significantly stronger visibility amplitude. The higher the amplitude, the more dominated we are by low fringe rates, which makes sense since there is a stronger DC component dominating over sky fringes. Figure 5 shows an example for this for a number of baselines with different visibility amplitudes.

Finally, the visibilities from select baselines with strong DC components were taken and a fringe rate spectrum was calculated for every 20 min of data. For the four hour observation this provides 11 data points² showing how the DC component varies with time. Figure 6 shows the time variability of baselines 229-203 and 215-260. Baseline 229-203 is an example for a baseline with low DC component amplitude showing little variation over the four hour period. Whereas baseline 215-260 shows a strong variability in the DC component values

²Some data was removed at the beginning and the end of the observation.

ranging from 200 - 1500. This variability provides additional evidence for the occurrence of strong DC components being externally driven.

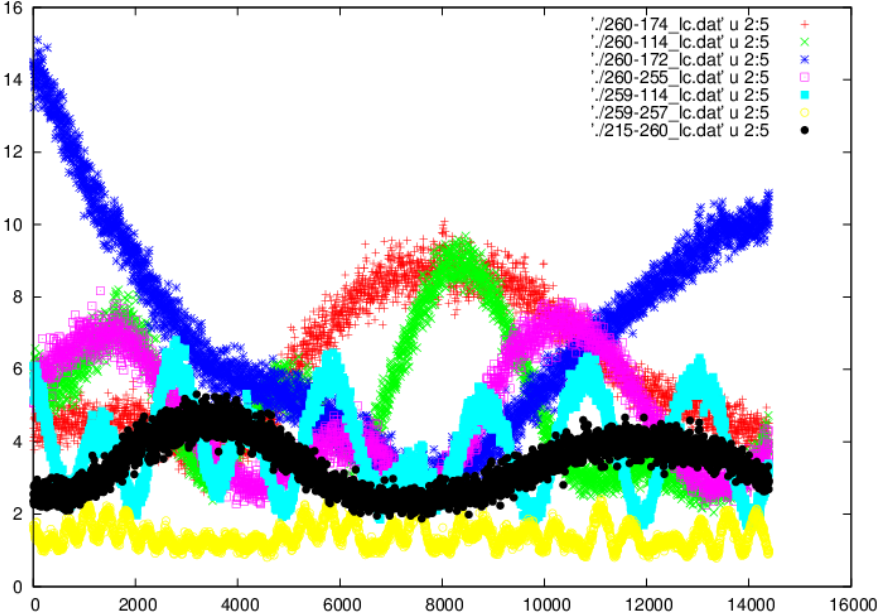


Figure 5: Visibility amplitudes (linear a.u.) against time (s) for a subset of baselines showing different visibility amplitudes. The less structure and the higher the amplitude, the higher is the DC component.

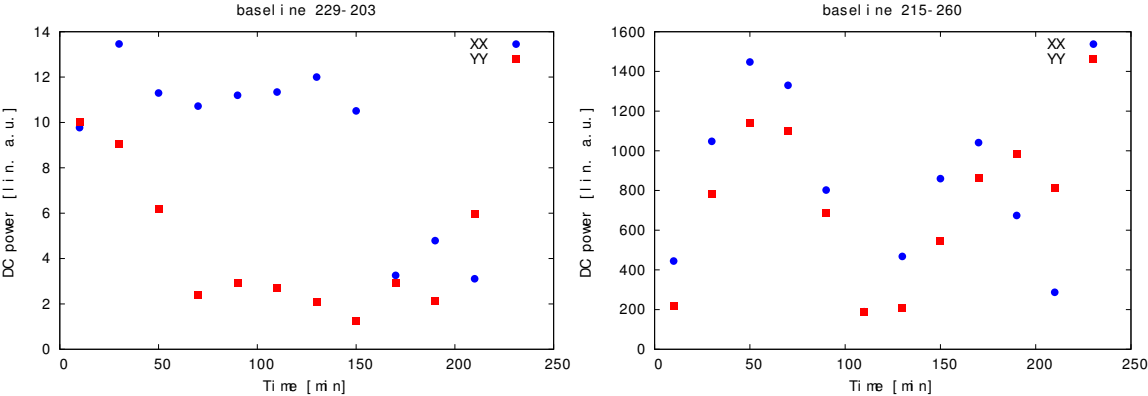


Figure 6: Left: Time variability of the DC component for baseline 229-203. Right: Time variability of the DC component for baseline 215-260.

4 Additional Observations from November 22 2013

Another set of four hour TBN observations was collected on November 22, 2013 between UT 02:03 and 06:03 (19:00 – 23:00 MST) at 37.89 MHz. In addition DRX data with the full sampling rate of 19.6 MSps for the single cross-dipoles, outrigger #1, #2, and #3 were recorded in order to search the data for powerline RFI. With difference to the previous October dataset, the November data was recorded with ASP in reduced bandwidth setting in order to reduce influence from low and high frequency RFI. The October dataset was recorded in split bandwidth mode and TBN data was recorded for 74 MHz. Analysis of the DC component for the LEDA64 baselines showed a much lower occurrence of high DC components compared to the dataset captured on October 31, 2013. However, high DC component amplitudes are still found on short baselines and some of the baselines that include stands #257 and #260, which translate to outriggers #1 and #2 and showed especially high DC components in the October 31 dataset as well.

In order to efficiently search the single dipole DRX data for powerline RFI and its variability, the frequency spectrum of the time series data were used to create a periodogram that is sensitive to repeating signals such as powerline RFI. In order to do so, 1 s of DRX timeseries data was taken and Fourier transformed using a Python wrapper for the FFTW library (pyFFTW)³. The Fourier transformed time series of 10 s (10 spectra) are then averaged to increase the signal to noise ratio of the periodogram. An example of the resulting spectrum is shown in Fig. 7. If powerline RFI were present then the frequency spectrum should show peaks at multiples of 60 Hz. And indeed a clear peak at 120 Hz can be seen as well as a considerably weaker peak at 60 MHz.

The strength of the 120 Hz signal for every 10 s interval is extracted from the periodogram in order to obtain the time variability of the strength of powerline RFI and to identify possible periods of low powerline RFI in order to verify the dependence of high DC component values on the strength of powerline RFI. This was done for the entire dataset of four hours for the three outriggers for which DRX data was recorded. The resulting light curves are shown in Fig. 8. All of the plots show an increase in the 120 Hz signal during the beginning of the observation and tapering off after about 2.5 hours into the observation. There is also a strong RFI peak visible around 6000 s into the observation for the 50 MHz tuning of stands #257 and #259. The strong time variability of powerline RFI is curious and could have been correlated with environmental parameters. Inspection of weather station data reveals no clear correlation with wind, however the rain sensor registered a similarly shaped time variability between 19:30 (1800 s) and 22:00 (10800 s) MST, see Fig. 9. It matches remarkably well with what was observed from the outrigger dipoles. Thus the conclusion is that we can actually measure when it is raining and how much just by observing powerline RFI with LWA1.

³The wrapper pyFFTW turned out to be more efficient than the numpy implementation of a FFT. It still required ~24 hours to process the entire raw dataset for both polarizations and tunings.

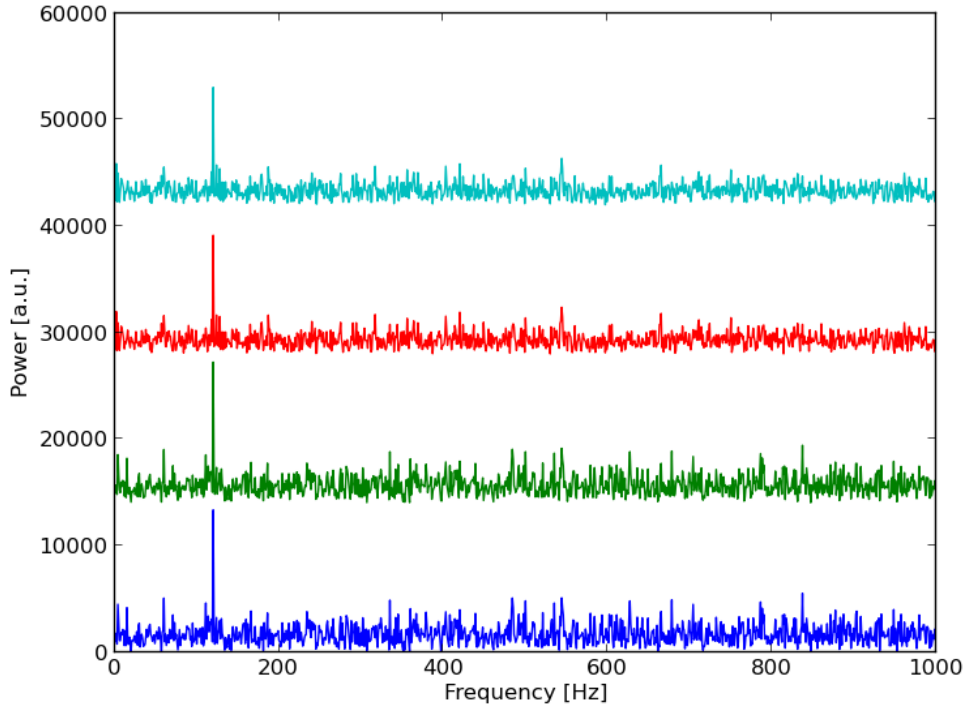


Figure 7: Averaged spectrum over 10 integration steps of 1 s integration each for outrigger #3. A peak at 60 Hz and 120 Hz shows up, with the one at 120 Hz being the strongest. The different curves representing two tunings and two polarizations are shifted with respect to each other for better readability. The curves represent from bottom to top Tuning 1 XX, Tuning 1 YY, Tuning 2 XX, and Tuning 2 YY, with Tuning 1 and 2 centered at 40 and 50 MHz respectively.

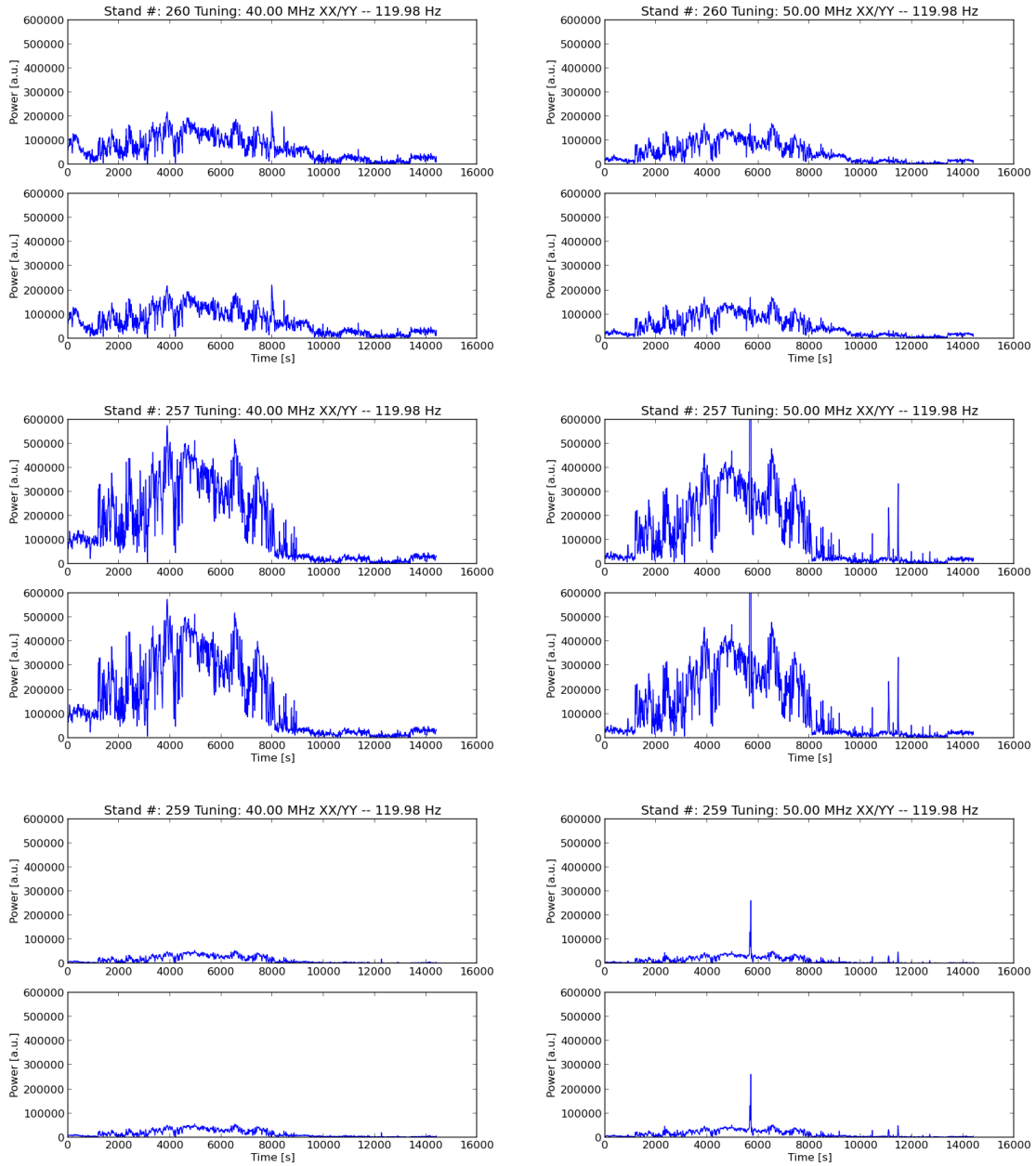


Figure 8: Time variability of the 120 Hz powerline RFI signal for outriggers #1, #2, and #3.

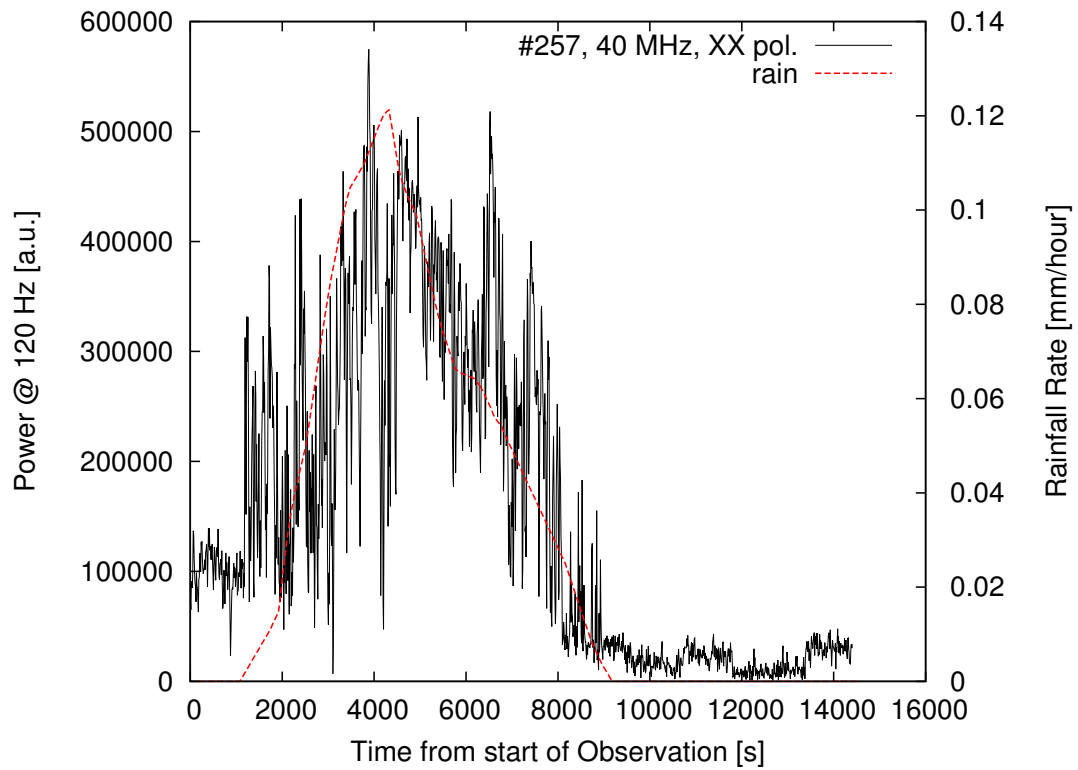


Figure 9: Direct comparison of the time variability of the 120 Hz powerline RFI signal of outrigger #1, 40 MHz tuning and XX polarization with the LWA1 weather station rain sensor data the same time period.

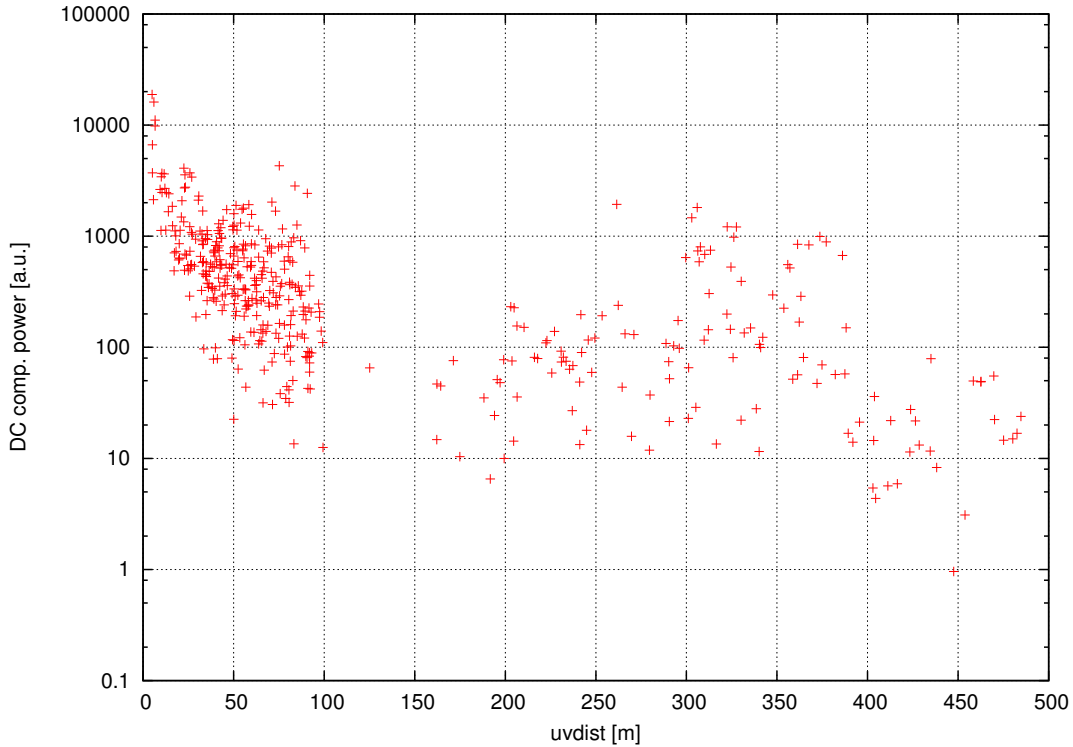


Figure 10: DC component values plotted against baseline length derived for the time period of low powerline RFI.

We can compare the peak values of power line RFI for all three outriggers. Outrigger #1 and #2 have similar cable lengths, whereas outrigger 3 has about a factor of 2 longer cable, which amounts to ~ 250 m, corresponding to an additional attenuation of 1.25 dB which is a power factor of 1.33. Thus, correcting for this, the 40 MHz peak values are:

- outrigger #1: 500000
- outrigger #2: 200000
- outrigger #3: 67000.

In conclusion outrigger #1 which shows the strongest powerline RFI signature is the closest to the VLA antenna assembly building (AAB). Faulty power equipment that is exposed to the weather could be causing the observed increase in powerline RFI.

Finally, the DC components for the low powerline RFI periods was extracted and is shown in Fig. 10. There is no evidence of common mode or significant signal cross-talk after removing adjacent channels. Also, the overall peak values of the DC components are much reduced over what was found on October 31, 2013.

5 Summary

Recent TBN observations show no unusually high DC component for most of the outrigger baselines given a correlated sky noise component. However, unusually high DC components were found initially in three baselines 257-260, 258-259, and 108-35. Further investigation of all LEDA64 baselines provides no evidence for a significant instrumental contribution to the DC component besides increased cross-talk for signals sharing the same RJ45 connector. Moreover, the only logical explanation that could be found for some of the strong DC components is of external nature.

Most affected by this are stand #257 (outrigger #1) and #260 (outrigger #2) and in particular E-W baselines. The possible source of this external interference are the powerlines running in E-W configuration providing power for LWA1 and the VLA.

In a subsequent observation in November 2013 the presence and time variability of powerline RFI was confirmed with outrigger #1 being the closest to the VLA AAB. Powerline RFI was identified to be stronger while it was raining at the site, correlating with the intensity of the rain recorded by the LWA1 weather station. Due to the fact that outrigger #1 is most affected, the source that is causing the RFI should be first searched in the vicinity of the AAB.

The DC components for all LEDA64 baselines were extracted for a period of low RFI that was identified from the dataset. After removal of baselines that have signals sharing the same RJ45 connection, the resulting distribution of DC components does not show significant outliers and especially high levels on long baselines.

Given the persistent and recurring presence of powerline RFI, despite continuing efforts by the observatory to mitigate it, it is recommended where possible (e.g. in raw DRX data) to excise data for powerline RFI if data quality is suspected to be compromised.

Known Issues with LEDA64 Stands

- Stand #123 dead Y polarization (update 11/21/13: bad ASP channel suspected)

Document Version History

- v1. 10/24/2013
- v2. 11/21/2013
- v3. 11/26/2013
- v4. 12/10/2013
- v5. 12/16/2013 – added comments by Jayce, significant changes to the figures etc.
- v6. 12/17/2013 – more minor changes, slight corrections to Table 1